In Situ, Time-Resolved Accelerator Grid Erosion Measurements in the NSTAR 8000 Hour Ion Engine Wear Test

J. E. Polk, J.R. Anderson, J. R. Brophy, V. K. Rawlin, M. J. Patterson, J. Sovey

Abstract

Time-resolved, in situ measurements of the charge exchange ion erosion pattern on the downstream face of the accelerator grid have been made during an ongoing wear test of the NSTAR 30 cm ion thruster. The measurements show that the pit and bridge depths vary linearly with time and that the wear rates are much lower than expected. The pit erosion rate decreases slightly with radius in the center part of the grid, while the bridge erosion rate is approximately constant. The groove width is constant in time, but increases with radius, confirming an important modeling assumption. The measured eroded area fraction is consistent with previous measurements obtained under identical conditions, while the erosion rates are lower by about a factor of three. This variability is not yet understood. The net sputter yield appears to be lower than that for normally incident ions striking the grid with an energy gained by falling through the full potential downstream of the grid. This suggests that a substantial fraction of the charge exchange production occurs in a region where the potential is negative of the beam potential.

Introduction

NASA's 30 cm xenon ion thruster technology is being validated for use in near-Earth and planetary missions in the NASA Solar Electric Propulsion Technology Application Readiness (NSTAR) program. A xenon ion primary propulsion system is one of the key technologies to be demonstrated in 1998 on Deep Space 1, the first of the New Millenium missions. Ion propulsion is also considered an enabling technology for the Champollion comet sample return mission, which was recently selected as the fourth New Millenium mission and is slated for launch in 2003. Ion thrusters are also being studied for use in a Europa Orbiter mission and in the Pluto Fast Flyby.

An important part of the NSTAR program is the assessment of the useful engine service life. Demonstrating engine reliability for the long operating periods required by planetary missions by testing alone would be prohibitively expensive, so lifetime assessment for engine wearout failure modes must rely to a large extent on analysis based on an understanding of the physics of failure. NSTAR is using a combination of analysis and testing to identify the dominant failure modes, develop and validate models of the physical wearout processes, characterize the uncertainties in the model input parameters and generate assessments of the failure risk as a function of service life by using wearout models in a probabilistic framework.

One potential failure mode is structural failure of the accelerator grid due to ion sputter erosion. A deterministic model of this failure mode was developed [1] and incorporated in a probabilistic analysis of failure risk [2]. This showed that the risk was dominated by lack of knowledge of certain model parameters. Time-resolved, in situ measurements of the erosion pattern are being made to verify model assumptions and provide information on input parameter values and their variability during an 8000 hour wear test being conducted under the NSTAR program. The grid structural failure model will first be reviewed, then the wear test conditions, experimental apparatus and results will be presented. Finally, the implications of the findings for wear modeling and failure assessment will be discussed.

Accelerator Grid Structural Failure Model

A number of sites on the accelerator grid that are subject to wear have been cataloged by Rawlin [3]. The dominant mass loss occurs in a series of pits and grooves surrounding each hole on the downstream surface and is highest in the center of the grid. Structural failure occurs when this pattern wears completely through the grid. Measurements of the erosion pattern on three grids showed that any model which relates structural failure to macroscopic parameters such as the total impingement current J_a must consider the detailed spatial and temporal distribution of wear [4]. The mass loss per unit area in the pits and grooves pattern in the grid center M''_{pg} can be expressed as

$$M''_{pg} = \left(\frac{m_g}{e(1-\phi_a)A_b}\right)\left(\frac{\lambda_Y \beta}{\alpha f_a}\right) J_a Y t, \qquad (1)$$

where m_g is the mass of a grid atom, e is the charge of an electron, ϕ_a is the grid open area fraction, A_b is the active beam area, t is the operating time and Y is the sputter yield for ions at normal incidence with an energy corresponding to the sum of the grid voltage, the coupling voltage and the beam potential relative to the ambient plasma potential. The parameter λ_Y is the ratio of the net sputter yield to Y and accounts for ions which do not fall through the entire potential in front of the grid, non-normal incidence, the presence of impurities on the grid and redeposition of sputtered material in the erosion pattern. The parameter β is the ratio of the total impingement current that is focused into the pits and grooves pattern, α represents the fraction of the webbing area covered by the erosion pattern and f_a is the mass loss flatness parameter, defined as the ratio of the average mass loss per unit area to the peak mass loss per unit area. This model essentially relates the total mass loss, which can be related to macroscopically observable parameters, to the mass lost in the pits and grooves pattern in the center of the grid, where structural failure occurs first. A failure criterion in the form of the mass loss per unit area at structural failure, which depends on the geometry of erosion, is coupled to Eq. (1) to calculate the time to failure. The measurements performed in the 8000 hour test are designed to verify the assumption that the eroded area fraction is constant in time, study how the rest of the pattern evolves in time and characterize the model parameters for the NSTAR thruster operating conditions.

The 8000 Hour Endurance Test

The objectives of this wear test are to identify any new potential failure modes, characterize wear processes to develop or improve models used in service life assessment and determine how engine performance varies with operating time. The endurance test is being conducted with the second Engineering Model Thruster (EMT2), fabricated by the Lewis Research Center (LeRC)[5, 6]. The thruster is operating at the full power level of 2.3 kWe with a beam current of 1.76 A, a beam supply voltage of 1100 V and an accelerator grid voltage of -180 V. The impingement current throughout the test has been about 6.5 mA. The coupling voltage has averaged 12.8 V and the measured beam potential relative to ground peaks at about 5 V. The facility and operating conditions are described in more detail in [7]. The engine has accumulated over 7400 hours of operation in this ongoing test and continues to operate remarkably well.

Characterization of the Erosion Geometry

Experimental Apparatus

The erosion pattern is measured using a Cyberoptics PRS-40 laser profilometer, which measures elevation changes over a 410 micron range with a resolution of 1 micron at a standoff distance of 1.89 cm. The laser profilometer is scanned across the surface using a 2-axis, stepper motor-driven positioning system which has a step size of 0.25 microns in each axis. The laser spot is visible on the grid surface, so a small video camera mounted with the sensor is used to specify the scan path. The profilometer, camera and positioning system are mounted on another positioning stage which is used to set the working distance from the grid. The system was aligned so that the limit switch on this positioning stage prevented moving the sensor any closer than about 3 mm from the face of the grid in the center to avoid inadvertantly touching the ion optics. Because of this requirement and the grid curvature, only the central portion of the grid within an 8 cm radius was accessibly with the profilometer. After 3100 hours of operation the failure

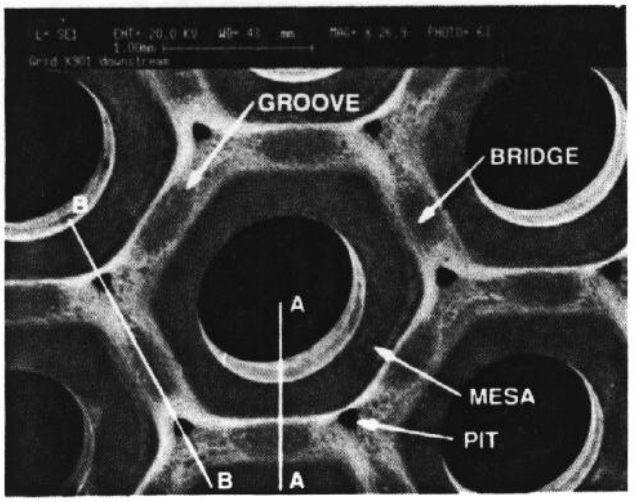

Figure 1: Characteristic form of accelerator grid erosion.

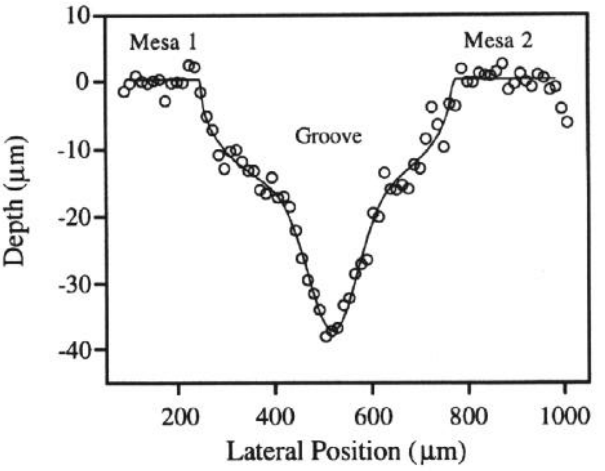

Figure 2: A-A scan across a groove near center hole at 6036 hours.

of a leveling motor on the thrust stand on which the thruster is mounted resulted in a slight movement of the engine upstream, further restricting grid profilometry to within a 5.3 cm radius of the center. The entire assembly is mounted on a fourth, larger positioning stage which is used to move the apparatus out of the beam when the engine is on. During engine operation the profilometer platform is enclosed in a box to prevent contamination of the optics by backsputtered material.

Procedures

Erosion measurements are performed approximately every 1000 hours. The calibration of the profilometer is first checked by scanning a calibration target mounted in the box in which the system is parked. Five precision-ground ceramic blocks with thicknesses accurate to within .05 microns were rung onto an optical flat to provide a series of steps of known height. The measurements show no drift in calibration and demonstrate that the sensor reading is accurate to within a few microns.

The erosion pattern is characterized at the center hole and at every sixth hole along a radius. The photomicrograph in Fig. (1) shows the pits and grooves pattern. This photograph is from a grid with pits which had worn completely through the thickness; however, in this test the pits have not yet penetrated the grid. Two scan paths denoted by A-A and B-B in the photo are used to characterize the pattern.

Because of the grid curvature, the surface is not in general parallel to the scan path, so the measured profiles are leveled digitally. Figure (2) shows the characteristic shape of the groove along the A-A path. These profiles can be fit very well using the sum of a Gaussian profile and a Beta distribution. The depth of the bridge is the difference between the level of the mesa and the minimum in the fit. The standard deviations of these two measurements yield an uncertainty of about 2.1 microns in the depth measurement. The width of the groove is determined from the left and right bounds of the Beta distribution, which are fit parameters with calculated uncertainties. The uncertainty in the width varies from 1 to 200 microns, depending on the quality of the fit. The fitting function is integrated numerically to determine the cross-sectional area of the groove. Estimates of the error associated with this calculation range from about 20 percent at the beginning of the test to about 5 percent in the latest measurements.

An example of a scan across two pits and along the floor of the groove between them (path B-B) is shown in Fig. (3). Reflections often lead to spurious readings on the steep walls of the pits, but good profiles of the mesas, pit floors and groove floors are obtain-

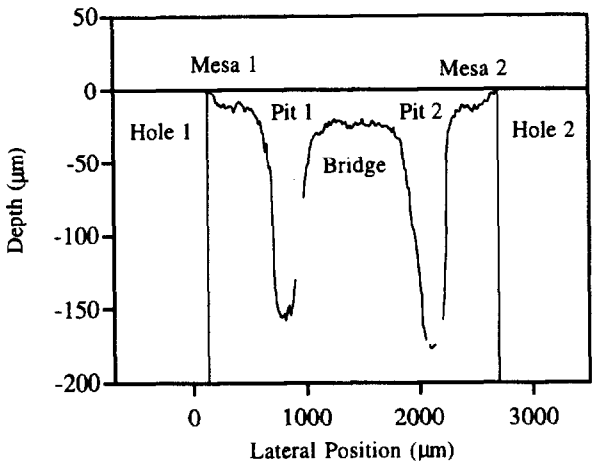

Figure 3: B-B scan across pits and groove near center hole at 4995 hours.

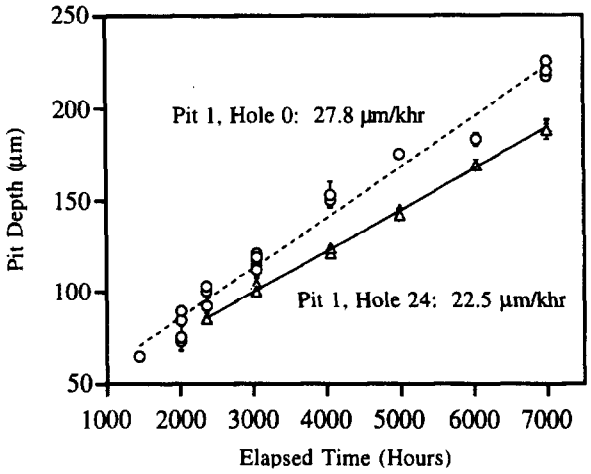

Figure 4: Examples of pit erosion rates calculated from depth vs time data.

able. The B-B profiles often show evidence of mesa erosion, which makes it difficult to discern a zero reference line, whereas the A-A profiles generally have relatively flat mesas. Therefore, the zero reference line for the B-B profiles is sometimes defined to give a bridge depth equal to that measured in the scan across the bridge. The pit depth is measured from the zero reference line with uncertainties that range from 2 to 7 microns. The floor diameter and upper diameter of the pits are measured to calculate the approximate pit volumes assuming they can be represented by truncated cones, and the length of the bridge between the cones is multiplied by the bridge cross-sectional area to estimate the groove volume. The uncertainty in these measurements was not calculated, but probably does not exceed to 5-20 percent uncertainty in the groove cross-sectional area.

Experimental Results

The pit depth was found to vary linearly with time in measurements from 1446hours to the latest measurements at 6999 hours for all pits examined. Examples of these results are shown in Fig. (4). In general the measurement uncertainties are smaller than the symbol sizes. The pit depth varies around any given hole, as the profile in Fig. (3) shows and also with radial position. The pit erosion rates based on weighted linear regression of the depth as a function of time were averaged for each radial position and plotted in Fig. (5). This shows that the pit erosion rate decreases with radius. The pit depth, however, does not decrease monatonically with radius, but peaks at the 4 cm radius, as shown in Fig. (6). This pattern was established before the 2365 hour measurements however, and has persisted since then because the erosion rates do not vary dramatically over this area of the grid. The dark bars on Fig. (5) represent the standard deviation of the measurements around the hole, while the thinner bars are the average standard deviations of the slopes from the individual linear fits. The dark bars therefore represent spatial variability and the thinnner ones the uncertainty in the rate measurements.

The bridge depth as a function of time was also found to be linear in all cases, indicating a constant erosion rate. The mean erosion rates as a function of radial position are shown in Fig. (7) and are approximately constant over this portion of the grid. Again, the bridges are deepest at a radius of 3–4 cm even though the erosion rate from 1446 hours to the latest measurements has been approximately constant. The groove width was found to be approximately constant in time. The weighted average of the widths measured at each radial position is plotted in Fig. (8), which shows that the groove width increases with radius. In this case the dark bars represent the variability of the groove width around the hole as well as variations in time. The thinner bars represent the uncertainty in any individual measurement.

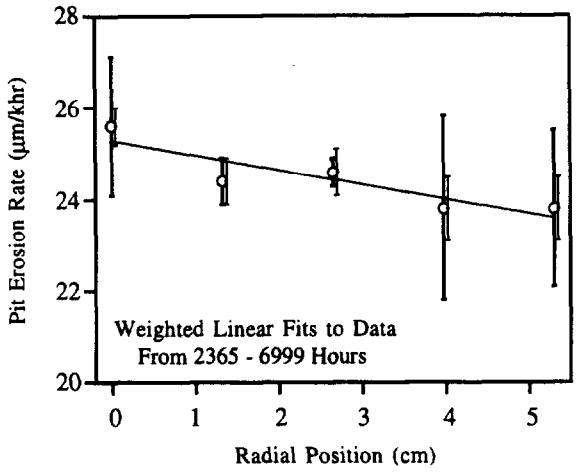

Figure 5: Radial variation in the pit erosion rate for the period 2365-6999 hours.

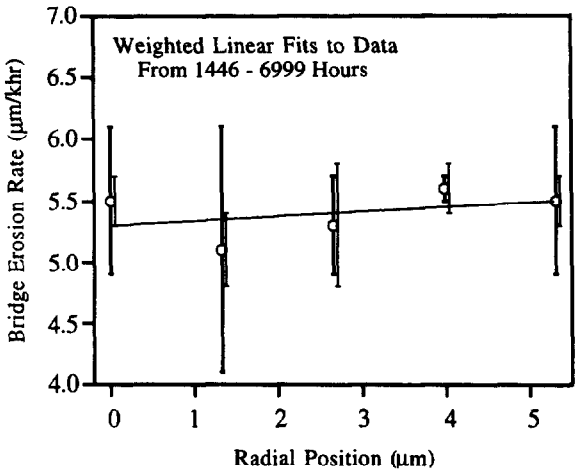

Figure 7: Radial variation in the depth erosion rate for the period 1446-6999 hours.

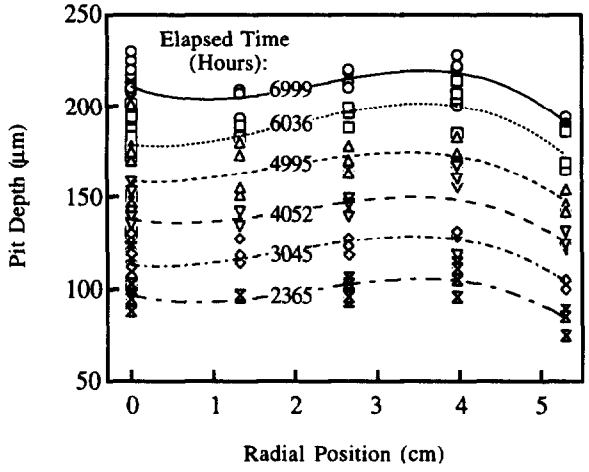

Figure 6: Radial variation in the pit depths for the period 2365-6999 hours.

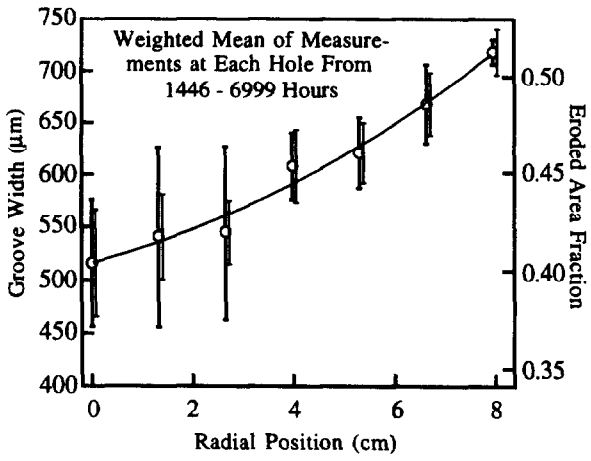

Figure 8: Radial variation in the groove width for the period 1446-6999 hours.

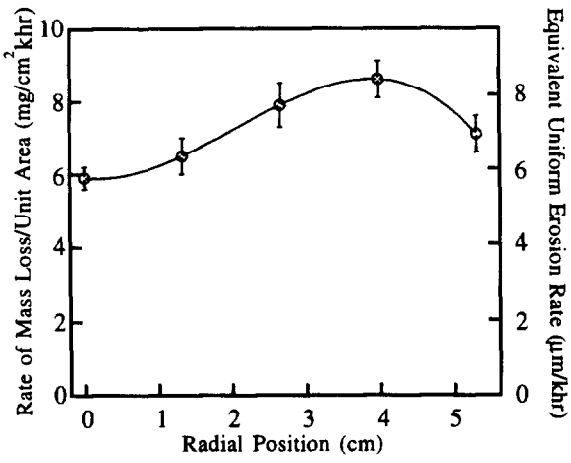

Figure 9: Radial variation rate of mass loss per unit area.

The approximate pit and groove volumes were multiplied by the density of molybdenum and then divided by the area covered by the pit and groove pattern to estimate the mass loss per unit area, M''_{pg}. This parameter was also found to vary linearly with time from 1446 hours to the latest measurements at 6999 hours, indicating a constant wear rate in the pits and grooves pattern over this time period. The data for each radial position were fit with a line. The slope and standard deviation of the slope are plotted as functions of radial position in Fig. (9). The shape of this line mirrors the shapes of the pit and bridge depths as functions of radius, indicating that the mass loss is peaked off-center. Dividing the mass loss per unit area by the density yields an equivalent erosion rate that would be observed if the wear were uniformly distributed in the pits and grooves pattern, which is plotted on the right-hand axis.

Discussion

The erosion rates measured in this test are encouragingly low and suggest that the optics have considerably longer service life capability than expected. The equivalent uniform erosion rate of 6–8 microns/khr measured in the center of the grid implies that only about 10 percent of the mass in the pits and grooves pattern has been removed in the 7000 hours of operation in this test. To develop confidence in applying these results to other operating conditions or conditions in space the wear processes must be understood and modeled properly.

The model assumption that the groove width or eroded area fraction is constant in time is supported by these measurements. This is consistent with earlier measurements made during an accelerated wear test [1] and suggests that the focusing into the pits and grooves pattern does not change significantly if the operating conditions are held constant as in this test. The groove width or eroded area fraction variation with radius found in this test agrees with data obtained from three grids used in other long duration tests [4]. This probably occurs because the charge exchange ions are less focused in regions where the beam current density is lower. If this is true, a higher eroded area fraction and therefore longer service life capability (or propellant throughput capability) would be expected at throttled conditions with lower beam currents.

These data represent the first extensive database of time-resolved erosion rate measurements from a long duration test. The data confirm that the bridge and pit erosion rates are constant over the period extending from 1446 hours to 6999 hours, that the bridge erosion rate is roughly constant over the center portion of the grid within a 5 cm radius and that the pit erosion rate decreases slightly with radius over this area. The pit and bridge depth data suggest that an initial pattern which deviated from this behavior was established in the first 1500 hours of operation. It is not clear what could have caused the wear rate to peak off-axis, and unfortunately no profilometer data were obtained during this period.

These data provide valuable information on the primary lifetime drivers. Previous assessments of grid lifetime yielded very conservative results, reflecting the risk associated with a lack of knowledge about these parameters. The eroded area fraction was initially treated parametrically [2], because so little information was available. These data show an eroded area fraction of 0.41 at the grid center with an uncertainty in the measurements of about 0.02 and slightly higher variability in the measurements around any one hole. This is consistent with values of 0.41–0.46 measured from photographs of the grid used in an earlier 1000 hour test at the same operating condi-

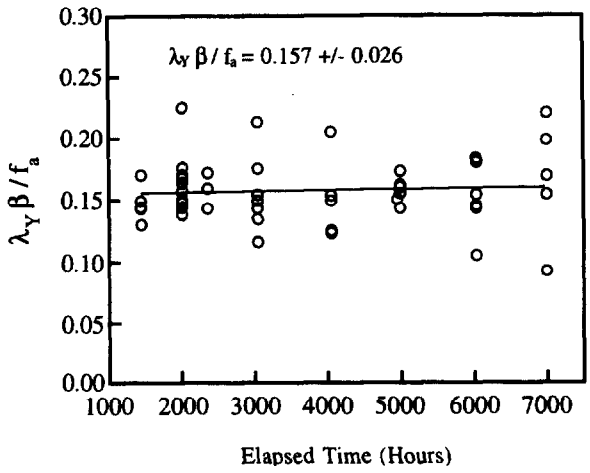

Figure 10: Variation of $\lambda_Y \beta / f_a$ during the test.

tions [8]. The model as originally proposed assumed that the eroded area fraction is constant over the surface of the grid [1]. The evidence that the eroded area fraction varies with radius does not invalidate the model; the model yields the proper mass loss per unit area in the center of the grid if the eroded area fraction for that region is used. Further modeling work is required to understand what determines the eroded area fraction and how sensitive it is to changes in the operating conditions.

The erosion rates measured in this test appear to have an uncertainty and spatial variability around the holes of about 5–10 percent. However, the pit and bridge erosion rates are about a factor of three lower than those measured at the end of the 1000 hour test performed under essentially identical conditions. This suggests either much larger stochastic variation than data from a single test would suggest, some uncontrolled factor which is different in the two tests or some systematic error in one or both measurement techniques.

The calculated mass loss per unit area can be used to estimate the magnitude of some of the important life drivers. Equation (1) can be solved for the ratio $\lambda_Y \beta / f_a$ as a function of constants and parameters measured in the test. This ratio for the center hole is plotted as a function of time in Fig. (10). This demonstrates that this ratio has remained constant at about 0.16 with an uncertainty of about 0.03 throughout the test. The mass loss flatness parameter is expected to be similar to the beam current flatness parameter of about 0.42 in space, but in ground tests is generally broadened. Previous measurements on other grids have yielded values of 0.61–0.89. The parameter β represents the fraction of impingement current which is focussed into the pits and grooves. Evidence of mesa erosion and accelerator grid hole enlargement [7] demonstrates that some fraction of the current is collected outside the pattern. From measured impingement currents and mass losses in the 1000 hour test, Brophy concluded that this factor was on the order of 0.75 [9]. The ratio β / f_a is therefore likely to be of order unity, implying that the net sputter yield is only about 15 percent of the published values for normal incidence at an energy of about 200 eV. This reduction could be due to redeposition of sputtered material in the pattern, a lower average ion energy than assumed or the effect of the deposition of carbon sputtered from the beam target onto the grid. The redeposition effect would be expected to increase in time as the erosion pattern grew deeper, but the data do not show this. Their is net carbon deposition on the grid periphery and on the mesas surrounding the holes, but there is no visible evidence of carbon deposits in the pits and grooves pattern. At this time, it seems most likely that the average ion energy is lower than 200 eV due to significant charge exchange production in regions where the local potential is negative with respect to the beam plasma. Further modeling and testing is required to confirm this conclusion.

Acknowledgements

The authors would like to acknowledge the invaluable fabrication and test support provided by LeRC's Test Installations Division as well as Al Owens, Bill Thogmartin and Bob Toomath at JPL. The support of other NSTAR Project members including Jack Stocky (JPL), Frank Curran and John Hamley (LeRC), Keith Goodfellow, Mike Marcucci, Dave Brinza, Mike Henry and Mike Smith (JPL) and Roger Myers (previously with NYMA, Inc.) is also gratefully acknowledged. The research described in this paper was conducted in part at the Jet Propulsion Laboratory, California Institute of Technology, and

was sponsored by the National Aeronautics and Space Administration.

References

[1] J.R. Brophy, L.C. Pless, and J. E. Polk. Test-to-Failure of a Two-Grid 30-cm Dia. Ion Accelerator System. In 23rd *International Electric Propulsion Conference*, Seattle, WA, 1993. AIAA-93-172.

[2] J.E. Polk, N.R. Moore, L.E. Newline, J.R. Brophy, and D.H. Ebbeler. Probabilistic Analysis of Ion Engine Accelerator Grid Life. In 23rd *International Electric Propulsion Conference*, Seattle, WA, 1993. AIAA-93-176.

[3] V.K. Rawlin. Erosion Characteristics of Two-Grid Ion Accelerating Systems. In 23rd *International Electric Propulsion Conference*, Seattle, WA, 1993. AIAA-93-175.

[4] J.E. Polk, J.R. Brophy, and J.Wang. Spatial and Temporal Distribution of Ion Engine Accelerator Grid Erosion. In 31st *Joint Propulsion Conference*, San Diego, CA, 1995. AIAA-95-2924.

[5] M.J. Patterson and T. Haag. Performance of the 30-cm Lightweight Ion Thruster. In 23rd *International Electric Propulsion Conference*, Seattle, WA, 1993. AIAA-93-108.

[6] J. S. Sovey et al. Development of an Ion Thruster and Power Processor for New Millenium's Deep Space 1 Mission. In 33rd *Joint Propulsion Conference*, Seattle, WA, 1997. AIAA-97-2778.

[7] J. E. Polk et al. The Effect of Engine Wear on Performance in the NSTAR 8000 Hour Ion Engine Endurance Test. In 33rd *Joint Propulsion Conference*, Seattle, WA, 1997. AIAA-97-3387.

[8] J.E. Polk et al. A 1000-Hour Wear Test of the NASA NSTAR Ion Thruster. In 32nd *Joint Propulsion Conference*, Lake Buena Vista, FL, 1996. AIAA-96-2717.

[9] J.R. Brophy, J.E. Polk, and V.K. Rawlin. Ion Engine Service Life Validation by Analysis and Testing. In 32nd *Joint Propulsion Conference*, Lake Buena Vista, FL, 1996. AIAA-96-2715.